THE JOURNAL OF BIOLOGICAL CHEMISTRY VOL. 286, NO. 19, pp. 17365–17375, May 13, 2011
Printed in the U.S.A.

Deficiency of Biglycan Causes Cardiac Fibroblasts to Differentiate into a Myofibroblast Phenotype*

Received for publication, October 11, 2010, and in revised form, February 2, 2011 Published, JBC Papers in Press, March 18, 2011, DOI 10.1074/jbc.M110.192682

Ariane Melchior-Becker[‡], Guang Dai[‡], Zhaoping Ding[§], Liliana Schäfer[¶], Jürgen Schrader[§], Marian F. Young[‖], and Jens W. Fischer[‡1]

From the [‡]Institut für Pharmakologie und Klinische Pharmakologie, Universitätsklinikum Düsseldorf, Heinrich-Heine-Universität Düsseldorf 40225, Germany, the [§]Institut für Herz- und Kreislaufphysiologie, Heinrich-Heine-Universität Düsseldorf 40225, Germany, the [¶]Pharmazentrum Frankfurt, Institut für Allgemeine Pharmakologie und Toxikologie/ZAFES, Klinikum der JW Goethe-Universität Frankfurt am Main 60590, Germany, and the [‖]Craniofacial and Skeletal Diseases Branch, NIDCR, National Institutes of Health, Bethesda, Maryland 20892

Myocardial infarction (MI) is followed by extracellular matrix (ECM) remodeling, which is on the one hand required for the healing response and the formation of stable scar tissue. However, on the other hand, ECM remodeling can lead to fibrosis and decreased ventricular compliance. The small leucine-rich proteoglycan (SLRP), biglycan (bgn), has been shown to be critically involved in these processes. During post-infarct remodeling cardiac fibroblasts differentiate into myofibroblasts which are the main cell type mediating ECM remodeling. The aim of the present study was to characterize the role of bgn in modulating the phenotype of cardiac fibroblasts. Cardiac fibroblasts were isolated from hearts of wild-type (WT) *versus* bgn$^{-/0}$ mice. Phenotypic characterization of the bgn$^{-/0}$ fibroblasts revealed increased proliferation. Importantly, this phenotype of bgn$^{-/0}$ fibroblasts was abolished to the WT level by reconstitution of biglycan in the ECM. TGF-β receptor II expression and phosphorylation of SMAD2 were increased. Furthermore, indicative of a myofibroblast phenotype bgn$^{-/0}$ fibroblasts were characterized by increased α-smooth muscle actin (α-SMA) incorporated into stress fibers, increased formation of focal adhesions, and increased contraction of collagen gels. Administration of neutralizing antibodies to TGF-β reversed the pro-proliferative, myofibroblastic phenotype. *In vivo* post-MI α-SMA, TGF-β receptor II expression, and SMAD2 phosphorylation were markedly increased in bgn$^{-/0}$ mice. Collectively, the data suggest that bgn deficiency promotes myofibroblast differentiation and proliferation *in vitro* and *in vivo* likely due to increased responses to TGF-β and SMAD2 signaling.

Cardiac fibroblasts are the main population of non-myocyte cells that maintain the structural integrity of the heart muscle by establishment and maintenance of the extracellular matrix (ECM).[2] In response to injury, cardiac fibroblasts infiltrate the ischemic area to initiate healing and scar formation. Cardiac ECM remodeling is affected by inflammation, hemodynamics, and pressure load and determines ventricle size, ventricle shape, and wall thickness eventually leading to ventricular dilation, infarct expansion, and heart failure (1). During cardiac remodeling fibroblasts differentiate into myofibroblasts, a fast proliferating, α-smooth muscle cell actin (α-SMA)-positive cell, with pronounced contractile and secretory properties (2–7). Myofibroblasts are the key cell type that reorganizes ECM and thereby confers adaptation to injury such as acute myocardial infarction (MI) (8). During cardiac remodeling, extensive *de novo* synthesis and degradation of ECM as well as a shift of the gene expression profile of ECM genes occurs (9). Myofibroblasts are not present in the healthy myocardium. Upon injury, myofibroblast differentiation is induced by pro-fibrotic growth factors such as TGF-β and supported by ECM such as fibronectin ED-A, which become thereby key players in infarct healing (10). Chronic or repeated injury of cardiac tissue may lead to persistence of more myofibroblasts contributing to cardiac fibrosis. Of note, particularly after cardiac injury myofibroblasts persist much longer after healing as compared with other tissues, which might in part be caused by the mechanical load through heart contraction and relaxation (11, 12).

In vitro upon treatment with pro-fibrotic growth factors such as TGF-β fibroblasts produce increasing amounts of ECM components including small leucine-rich repeat proteoglycans (SLRP) such as biglycan (bgn) (13) and decorin. Bgn and decorin are key regulators of lateral assembly of collagen fibers. Deficiency of one or more SLRPs leads to abnormal collagen fiber diameters and disturbed lateral association of fibers (14, 15). In addition bgn is thought to be involved also in assembly of elastin fibers (16). In addition to its structural functions bgn is involved in growth factor signaling by sequestering growth factors in the ECM (17) and is itself a ligand and/or cofactor to receptors of innate immunity via binding to toll-like receptors (18). Furthermore, bgn is a ligand of CD44 (19), a cell surface receptor that is postulated to functionally interact with TGF-β in myofibroblast differentiation (20). With respect to cardiac pathophysiology, it is known that both SLRPs, biglycan, and decorin, are up-regulated during infarct healing (21, 22). Bgn-deficient male mice (bgn$^{-/0}$) experience increased mortality and impaired hemodynamic function after experimental MI and a higher incidence of ventricular ruptures. The underlying mechanism appears to be a distorted and fragile collagen scar in

* This work was supported by Deutsche Forschungsgemeinschaft Grant GRK 1089.

[1] To whom correspondence should be addressed: Institut für Pharmakologie und Klinische Pharmakologie, Heinrich-Heine-Universität Düsseldorf, Moorenstrasse 5, 40225 Düsseldorf, Germany. Tel.: 49-211-8112500; Fax: 49-211-81-14781; E-mail: jens.fischer@uni-duesseldorf.de.

[2] The abbreviations used are: ECM, extracellular matrix; MI, myocardial infarction; SMA, smooth muscle cell actin; bgn, biglycan; SLRP, small leucine-rich proteoglycan.

the absence of biglycan (22, 23). As myofibroblasts are the main players in establishing of the infarct scar the aim of this study was to elucidate the role of biglycan for phenotypic control of cardiac fibroblasts.

EXPERIMENTAL PROCEDURES

Animals and Surgical Procedures—Male bgn$^{-/0}$ mice with a targeted deletion of the bgn gene (24) and male wild-type littermates (WT, C57BL/6) were compared in this study. Animals were housed under standard conditions (55% humidity, 12 h day-night rhythm, standard chow, and water *ad libitum*). All procedures were carried out in accordance with the AAALAC guidelines and Guide for the Care and Use of Laboratory Animals (Department of Health and Human Services, National Institutes of Health, Publication No. 86-23) and were approved by the ethical and research board of the University and the county of Düsseldorf.

Primary Cardiac Fibroblasts—Murine cardiac fibroblasts were isolated from 6-week-old mice. Mice were euthanized by CO_2 inhalation. Skin was removed and the chest was opened with sterile instruments. The heart was freed from pericardium and atria were removed. Ventricles and septum were transferred into sterile PBS, washed twice in PBS, and cut into small pieces and transferred into 6-well culture plates. Culture plates were precoated with 5 μg of collagen type I/well (PureCol® Collagen, Nutacon). Cardiomyocyte-plating medium contained 60% FCS and 8 ng/ml basic fibroblast growth factor (bFGF). After 24 h, at 37 °C the plating medium was removed and DMEM containing 20% FCS and 8 ng/ml bFGF was added. Subsequently, the medium was changed every other day for a period of 2 weeks. For the first passage fibroblasts were washed twice with PBS and treated with trypsin for 10 min at 37 °C and transferred to a fresh culture dish. Two days later the medium was changed to DMEM containing 10% FCS, and cells were used for experiments after reaching confluence. Only the first three passages were used (13).

The yield of fibroblasts from these explant cultures was determined by cell counting after trypsin treatment (0.05% trypsin in 0.02% EDTA for 10 min). For most experiments fibroblasts were plated at 5000 cells/cm^2 and grown in media containing 2 or 5% FCS. All stimuli were added to DMEM media containing at least 5% FCS, without previously starving cells. Instead of serum withdrawal synchronization was achieved by trypsinization and plating. This was necessary because bgn$^{-/0}$ fibroblasts were very sensitive to serum depletion. A few experiments were performed after serum starvation as indicated. To assay proliferation viable cells were counted in the presence of trypan blue after trypsin treatment. DNA synthesis was determined by incorporation of [^{3}H]methyl-thymidine into newly synthesized DNA as described (25).

Proliferation on Cell-derived ECM—To determine the effect of ECM on proliferation primary fibroblasts were used to deposit the ECM on the culture dish. For this purpose the cells were fed with DMEM containing 10% FCS and 56 μg/ml ascorbic acid, which is known to stimulate collagen production and deposition (26–28). After 20 days, ECM was macroscopically visible on the plate. To obtain cell-free ECM, the cell layers were washed twice with PBS and lysed with 2.5 μM ammonium hydroxide (30 min, room temperature) (29–31). After lysis of the cells, the WT and bgn$^{-/0}$ ECM were washed three times with sterile distilled water and stored at 4 °C overnight. Subsequently, fibroblasts were plated on these cell-free ECM at a density of 10^3 cells per cm^2. The cells were allowed to settle and grow for 48 h. Afterward cell number was determined as described above.

TABLE 1
Primer for gene expression analysis

Gene	Primer sequence
α-SMA	5′-CAGGCATGGATGGCATCAATCAC-3′, 5′-ACTCTAGCTGTGAAGTCAGTGTCG-3′ (33)
TGF-β1	5′-CCGCAACAACGCCATCTATG-3′ 5′-CTCTGCACGGGACAGCAAT-3′
TGF-βRII	5′-CAAGTCGGATGTGGAAATGG-3′, 5′-AAATGTTTCAGTGGATGGATGG-3′
CD44	5′-AGGATGACTCCTTCTTTATCCG-3′, 5′-CTTGAGTGTCCAGCTAATTCG-3′
PLOD1	5′-GAGCCTTGGATGAAGTTGTG-3′ 5′-TAGTTGCCCAGGTAGTTCAG-3′
PLOD2	5′-AGTGGCAATTAATGGAAATGGG-3′, 5′-CTTGGGAGGGACATCTACTG-3′
mmp13	5′-GATGACCTGTCTGAGGAAGACC-3′ 5′-CAAGAGTCGCAGGATGGTAGT-3′
Paxillin	5′-AATTCCAGTGCCTCCAACAC-3′ 5′-GGAGGAGCTCATGACGGTAG-3′
Vinculin	5′-CGGGTTGGAAAAGAGACTGT-3′ 5′-GGAACCGAGTATGGGTCTGA-3′
SMAD7	5′-GCATTCCTCGGAAGTCAAGA-3′ 5′-GAGTAAGGAGGAGGGGGAGA-3′

Lentiviral Overexpression of bgn—The cDNA of murine bgn was amplified by RT-PCR using the total RNA extracted from hearts of C57/Bl6J mice. Amplification was achieved using the primers as follows: XhoI-mBGN-F 5′-CTCGAGATGTGTCCCCTGTGGCTACTC-3′ and EcoRI-mBGN-R 5′-GAATTCCTACTTCTTATAATTTCCAAA-3′. The cDNA was cloned into the pCL1mcs vector (32, 33) using XhoI and EcoRI restriction sites. The production of lentivirus, harvest of recombinant lentiviral particles, and transduction of primary murine cardiac fibroblasts were performed as previously described (34). In this lentiviral vector, the CMV promoter drives the overexpression of biglycan. The pCL1 vector expressing only EGFP was used as mock control. Transfected fibroblasts were used 7 days after transfection.

Purified Biglycan—To reconstitute the bgn content, human biglycan was purified as described previously (35–37) and added to collagen type 1 (PureCol Collagen, Nutacon) at 0.5 μg/ml prior to coating of cell culture plates. Subsequently, cell proliferation was determined by cell counting.

Immunocytochemistry—To analyze cell morphology fibroblasts were plated on LabTek^{TM} cell culture microslides (Nunc). After incubation under standard conditions the cells were washed and fixed by PBS-buffered paraformaldehyde (3.7%) for 20 min at room temperature. Afterward, the cells were incubated with the primary antibody for 1 h at room temperature and washed again five times before the fluorochrome-conjugated secondary antibody was added (1 h, room temperature). Nuclei were stained by HOECHST Dye (1:10,000; Invitrogen) for 5 min in the dark, and specimens were embedded with Vectashield (Vector Labs) mounting medium.

Oil-supported Collagen Gel Retraction Assay—This assay was performed as described by Vernon and Gooden (38) using 1.25 mg/gel of PureCol® Collagen (Nutacon). This assay visu-

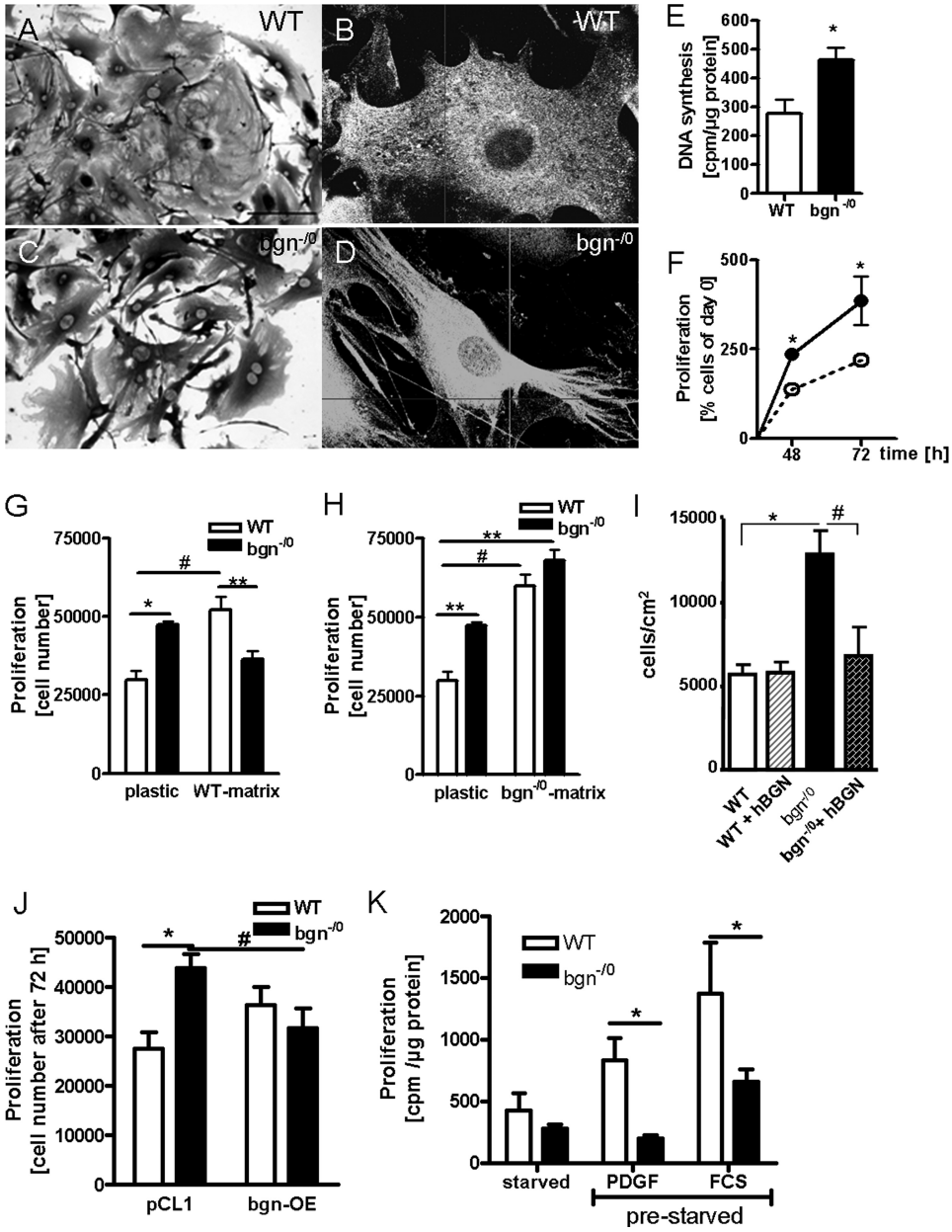

FIGURE 1. **Lack of bgn causes increased proliferation of cardiac fibroblasts.** *A–D*, morphology of WT (*A* and *B*) and bgn$^{-/0}$ cardiac fibroblasts (*C* and *D*). *A* and *C*, 200× and *C* and *D*, 400× magnification. *E*, DNA synthesis as measured by [H^3]thymidine incorporation at 24 h in response to 5% FCS was increased in bgn$^{-/0}$ fibroblasts; $n = 5$ (WT), $n = 4$ (bgn$^{-/0}$). *F*, proliferation as determined by cell counting after 48 and 72 h under standard culture conditions (5% FCS) was increased in bgn$^{-/0}$ fibroblasts; $n = 4$ (48 h), $n = 6$ (72 h). *G* and *H*, effects of cell-free ECM derived from WT *versus* bgn$^{-/0}$ fibroblasts on proliferation of cardiac fibroblasts. Fibroblasts were plated on either plastic or WT fibroblast ECM (*G*) or bgn$^{-/0}$ fibroblasts-derived ECM (H) and grown for 48 h in 5% FCS; $n = 4$. *I*, cell proliferation as determined by cell counting in WT and bgn$^{-/0}$ fibroblasts on collagen matrix plus and minus purified human bgn, $n = 4$. *J*, lentiviral overexpression of bgn in bgn$^{-/0}$ fibroblasts inhibited proliferation to WT level; cell counts after 72 h; $n = 4$. *K*, stimulation with either PDGF-BB (10 ng/ml) or 10% serum (FCS) failed to stimulate DNA synthesis in bgn$^{-/0}$ fibroblasts after serum withdrawal; $n = 12$ (starved), $n = 4$ (PDGF), $n = 6$ (FCS). Data are presented as mean ± S.E.; * and #, $p < 0.05$; **, $p < 0.01$.

alizes the ability of cells to contract collagen matrices that are free of adhesion. 12-well cell culture plates contained 1.4 ml sterile mineral oil and a polyethylene (PE) ring on a Teflon® disk to allow adhesion-free polymerization of collagen gels. The cell-collagen solution was added to the inner circle of the PE ring and polymerized for 2 h at 37 °C and 5% CO_2. After 24 h, gel images were recorded under dark field illumination, and the size of the gels was determined by ImageJ (NIH).

mRNA Expression—Total RNA was extracted from cell cultures and the apex of hearts using TRIzol reagent (Invitrogen) according to the manufacturer's instructions. The synthesis of cDNA by reverse transcriptase using random hexamer primers was performed with 1 μg of total RNA using the Quantitect reverse transcription kit (Qiagen). Relative quantitation of mRNA expression levels were performed by qPCR with ABI 7300 real time system (Applied Biosystems) using Platinum SYBR green qPCR SuperMix-UDG kit (Invitrogen). Glyceraldehyde-3-phosphate dehydrogenase (GAPDH) is constitutively expressed and was chosen as endogenous control. PCR amplification was performed at initially 50 °C for 2 min, fol-

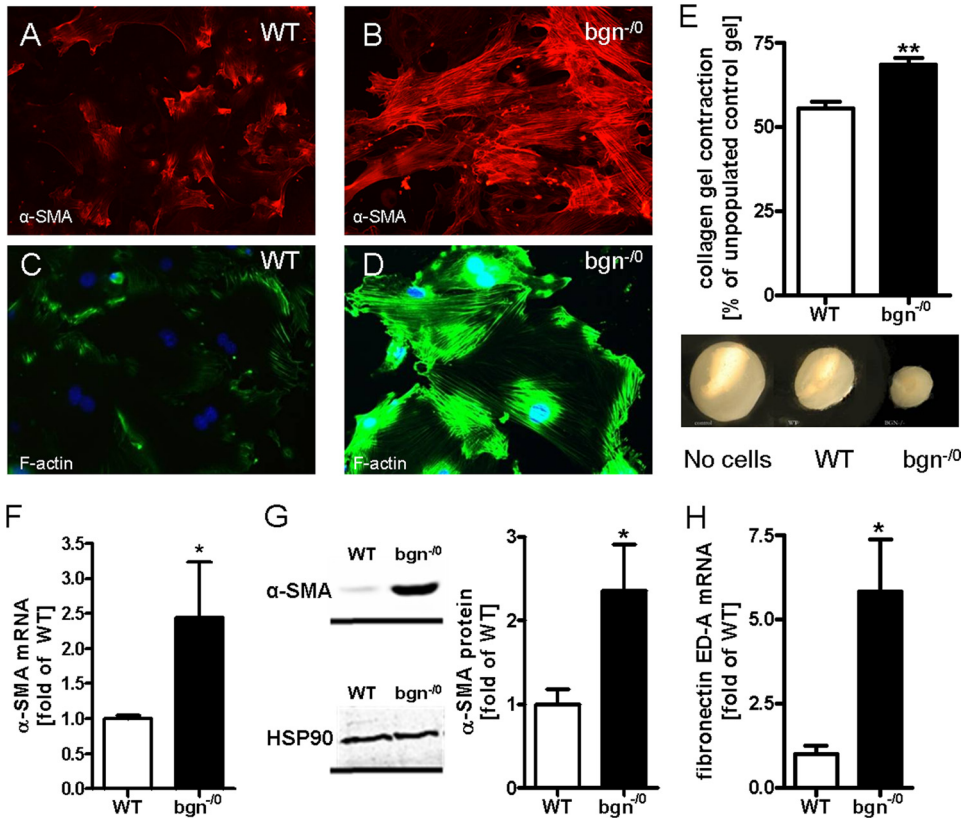

FIGURE 2. **Cardiac fibroblasts derived from bgn$^{-/0}$ mice displayed characteristic features of differentiated myofibroblasts.** *A* and *B*, immunocytochemical staining of α-SMA in WT (*A*) and bgn$^{-/0}$ fibroblasts (*B*) at 200 × magnification. *C* and *D*, immunostaining of F-actin at 200 × magnification. *E*, collagen gel contraction by bgn$^{-/0}$ fibroblasts was increased after 24 h; $n = 4$. mRNA expression of α-SMA is elevated in bgn$^{-/0}$ fibroblasts, $n =$ xy. *G*, α-SMA and HSP90 immunoblotting. Quantitative analysis was achieved by the ratio of α-SMA and HSP90 to control for loading, $n = 5$. *H*, mRNA expression of fibronectin ED-A fragment was significantly induced in bgn$^{-/0}$ fibroblasts; $n = 4$. Data are presented as mean ± S.E.; *, $p < 0.05$; **, $p < 0.01$.

lowed by 95 °C for 2 min and 40 cycles at 95 °C for 30 s and terminated by 60 °C for 30 s. Primer sequences are provided in Table 1.

Protein Analysis—Western blotting was performed using cell lysates of 10^5 cells under standard conditions (5% serum). Equal amounts of protein were run by standard 10% SDS-PAGE. HSP90, β-tubulin, and GAPDH were used as loading controls. Analysis was followed by incubation with primary antibodies. The following primary antibodies were from Cell Signaling: p44/42 MAPK (ERK1/2), phospho-p44/42 MAPK (pERK1/2), SMAD3 and phospho-SMAD3, SMAD2, and phospho-SMAD2. β-Tubulin antibody was from Sigma-Aldrich. HSP90, GAPDH, and SMAD7 primary antibodies were from Santa Cruz Biosciences. IR-Dye-conjugated secondary antibodies were used for visualizing and quantifying protein levels with the Odyssey Near Infrared Imaging System (Licor Biosciences).

TGF-β ELISA was obtained from R&D Systems and was performed according to the manufacturer's instructions to analyze cell culture supernatants. All samples were normalized to non-conditioned media.

Experimental Myocardial Infarction—At the age of 12 weeks, WT and bgn$^{-/0}$ mice were anesthetized by *i.p.* injection of pentobarbital (100 mg/kg). A 2-cm long PE-90 catheter attached to the hub of a needle was inserted into the trachea. To numb the throat and reduce gag reflex a drop of 1% lidocaine was put on the tip of the tube. Mice were subjected to permanent LAD-occlusion followed by recovery for 3 or 7 days as described before (22). Infarcted left ventricles were used for immunoblotting and total RNA was isolated from the apex. For immunohistochemistry hearts were immediately placed in cryomolds with OCT-Medium and frozen in liquid isopentane at 40 °C. All procedures were carried out as recently described in detail (39).

Immunohistochemistry—Cross sections of infarcted left ventricles were prepared from native frozen tissue. Cryosections (10 μm) were cut at −25 °C using a Leica cryostat. Cryosections were fixed in absolute ethanol at 4 °C and rehydrated (5 min) in 70% ethanol at 4 °C. Subsequently, sections were washed with PBS and incubated for 1 h at room temperature in blocking solution (3% BSA in PBS). Incubation with primary antibodies was performed over night (4 °C). Blocking of endogenous peroxidases was performed in 3% H_2O_2 for 20 min at room temperature prior to incubation with HRP-conjugated secondary antibody (1 h, room temperature). Detection with DAB solution was performed for 10 min at room temperature and followed by counterstaining of nuclei with Mayer's Hematoxylin.

RESULTS

Pro-proliferative Phenotype of Primary Cardiac Fibroblasts from bgn$^{-/0}$ Mice—WT fibroblasts were well spread and displayed few plasma membrane protrusions (Fig. 1, *A* and *B*). In contrast, bgn$^{-/0}$ fibroblasts were characterized by numerous protrusions of the cytoplasm creating an irregular cell shape (Fig. 1, *C* and *D*). In explant cultures, the number of cells that grew out was significantly increased in bgn$^{-/0}$ (data not shown)

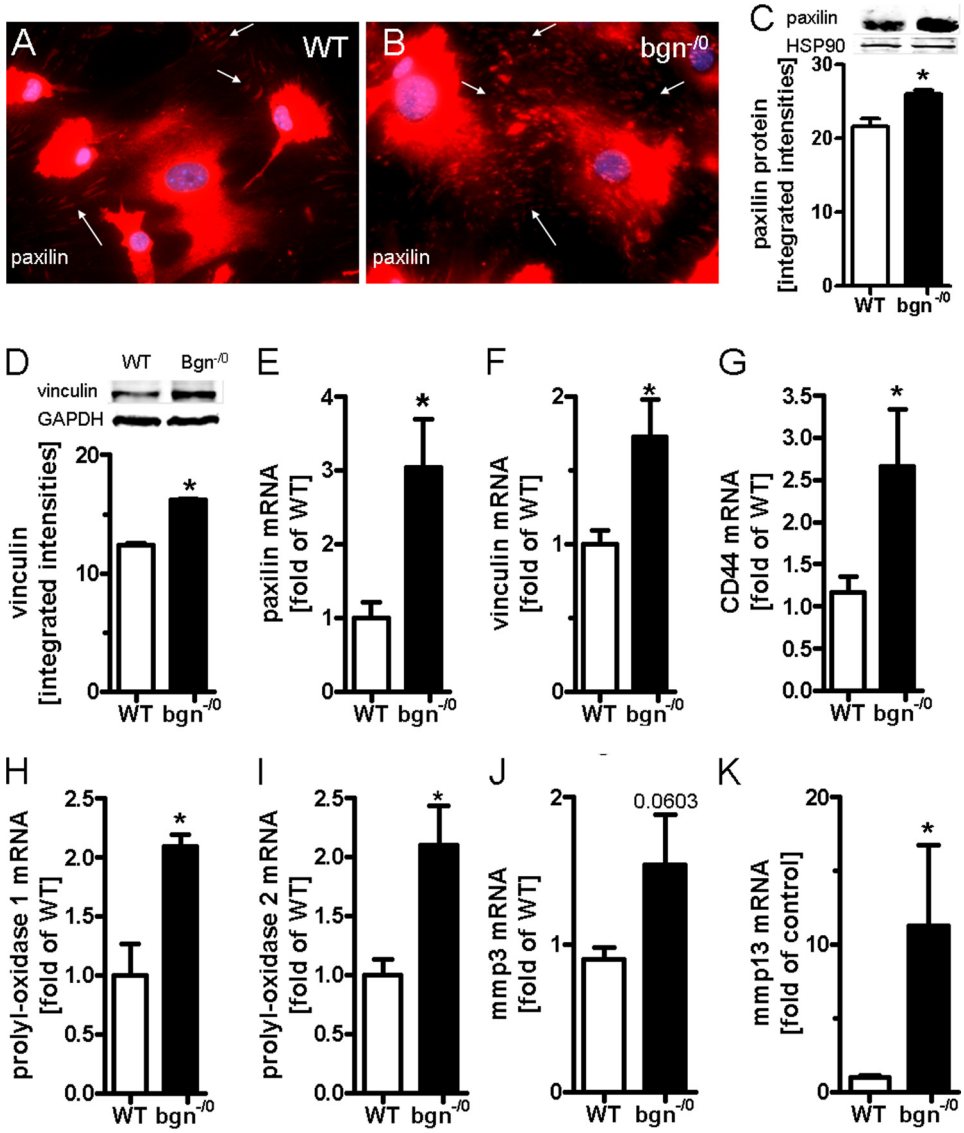

FIGURE 3. **Increased focal adhesions and differential regulation of ECM-related genes in bgn$^{-/0}$ myofibroblasts.** *A* and *B*, immunocytochemical analysis of paxillin revealed increased establishment of focal adhesions (*FA*) in bgn$^{-/0}$ fibroblasts. FA are pointed out by *white arrows*. *C–F*, immunoblotting and mRNA expression of paxillin and vinculin 24 h after plating in 5% FCS confirmed the results obtained by immunostaining, $n = 3$. *G–K*, mRNA expression of cell surface ECM receptor CD44, the ECM-modifying enzymes plod1 (*H*), plod2 (*I*), MMP3, and MMP13 24 h after plating in 5% FCS; $n = 3$ (PLOD1, 2); $n = 4$ (MMP3, 13). Data are presented as mean ± S.E.; *, $p < 0.05$.

suggesting a pro-proliferative phenotype and/or a pro-migratory phenotype. Furthermore, first passage fibroblasts had significantly increased DNA-synthesis as evidenced by [^{3}H]methyl-thymidine incorporation (Fig. 1*E*), which translated into increased proliferation as shown by growth curves (Fig. 1*F*). To investigate if the enhanced proliferation of bgn$^{-/0}$ fibroblasts was due to the lack of bgn in the pericellular matrix, bgn$^{-/0}$ fibroblasts were grown on WT cell-derived ECM and WT fibroblasts were grown on bgn$^{-/0}$ ECM. Providing WT cell-derived ECM as substrate to WT fibroblasts exhibited enhanced growth similar to bgn$^{-/0}$ fibroblasts on plastic (Fig. 1*G*). Importantly, providing bgn$^{-/0}$ fibroblasts with WT cell-derived ECM inhibited their growth to WT level on plastic (Fig. 1*G*). On the other hand using bgn$^{-/0}$ cell-derived ECM, fibroblasts of both genotypes showed increased growth and the difference between WT and bgn$^{-/0}$ fibroblasts was no longer detectable (Fig. 1*H*). To verify if this difference in proliferation is caused by the lack of bgn, recombinant human BGN protein was mixed with type I collagen and provided as ECM substrate to the primary cardiac fibroblasts. Whereas WT fibroblasts were not influenced by the substrate, bgn$^{-/0}$ fibroblasts were indeed inhibited to WT level (Fig. 1*I*). To further corroborate this key finding bgn expression was restored in bgn$^{-/0}$ fibroblasts by lentiviral transduction. Overexpression of bgn reduced the proliferation of bgn$^{-/0}$ fibroblasts to the level of WT fibroblasts treated with the control vector pCL1 (Fig. 1*J*). Another phenotypic facet of bgn$^{-/0}$ fibroblasts was that bgn$^{-/0}$ fibroblasts did not re-enter cell cycle after serum withdrawal as evidenced by the paucity of response to platelet-derived growth factor BB (PBGF-BB) and to 10% serum (Fig. 1*K*). Therefore all experiments were performed in the presence of serum.

Increased α-SMA Expression and Matrix Contraction by bgn$^{-/0}$ Fibroblasts—Immunocytochemistry (ICC) of the cytoskeleton revealed that bgn$^{-/0}$ fibroblasts displayed increased

α-SMA containing stress-fibers indicative for myofibroblasts (Fig. 2, *A–D*) (40). Additionally, bgn$^{-/0}$ fibroblasts contracted polymeric collagen gels more strongly compared with WT as revealed by OSCR assay (Fig. 2*E*). Increased expression of α-SMA was verified by qPCR and immunoblotting (Fig. 2, *F* and *G*). Another characteristic feature of activated fibroblasts is the expression of fibronectin ED-A fragment, which was analyzed by qPCR. In bgn$^{-/0}$ fibroblasts fibronectin ED-A fragment was strongly up-regulated (Fig. 2*H*). Other morphological hallmarks of myofibroblasts (40) are focal adhesions. Therefore, paxillin and vinculin (Fig. 3, *A–F*) were analyzed. mRNA and protein expression of both genes were significantly up-regulated in bgn$^{-/0}$ fibroblasts. CD44 is a surface receptor that is activated by bgn, hyaluronan, and osteopontin and is thought to support myofibroblast infiltration and differentiation (19, 20, 41–43) Interestingly, CD44 was significantly up-regulated in bgn$^{-/0}$ fibroblast (Fig. 3*G*) (42). With respect to secondary changes in the ECM bgn$^{-/0}$ fibroblasts showed significantly increased expression of enzymes involved in ECM remodeling such as the procollagen-lysyl-oxidases (PLOD) that crosslink collagen networks and ECM degrading enzymes such as MMPs. Specifically, PLOD1, PLOD2, and MMP13 were up-regulated (Fig. 3, *H–K*) (8).

The Phenotype of bgn$^{-/0}$ Fibroblasts Is Driven by TGF-β—Subsequently, the molecular mechanisms were addressed that were responsible for the myofibroblast phenotype of bgn$^{-/0}$ fibroblasts. Differentiation of fibroblasts into myofibroblasts can be induced by transforming growth factor β (TGF-β), fibronectin fragment ED-A, and mechanical tension (5). Therefore, first the response to TGF-β was addressed. Bgn$^{-/0}$ fibroblasts showed slightly reduced concentrations of free secreted TGF-β into cell culture supernatants (Fig. 4*A*) whereas mRNA expression of TGF-β was not different between the two genotypes (Fig. 4*B*). On the other hand the TGF-β receptor Type II (TGF-βRII) was significantly up-regulated in bgn$^{-/0}$ fibroblasts shown by qPCR and immunoblotting (Fig. 4, *C* and *D*). In addition immunocytochemistry confirmed increased TGF-βRII expression in bgn$^{-/0}$ fibroblasts (Fig. 4, *E* and *F*). Therefore, the possibility that increased signaling of endogenous TGF-β is responsible for the phenotype was analyzed in further detail.

Indeed, administration of a neutralizing antibody to TGF-β abolished the increased proliferation of bgn$^{-/0}$ fibroblasts. In contrast the neutralizing antibody had no effect on the proliferation of WT fibroblast (Fig. 5*A*). Furthermore, the increased collagen contraction by bgn$^{-/0}$ fibroblasts was abolished by the neutralizing TGF-β antibody as well (Fig. 5*B*). Likewise the neutralizing TGF-β antibody strongly reduced the expression of α-SMA in bgn$^{-/0}$ fibroblasts as evidenced by ICC (Fig. 5, *E* and *F*). The responsiveness of α-SMA to blocking TGFβ was confirmed by immunoblotting (Fig. 5*G*) and qPCR (Fig. 5*J*). Furthermore neutralization of TGF-β reduced paxillin, TGF-βRII, and fibronectin ED-A expression (Fig. 5, *H*, *I*, *K*, *L*).

Enhanced TGF-β Signaling and Apoptosis in bgn$^{-/0}$ Fibroblasts.—Because all key features of myofibroblast phenotype of bgn$^{-/0}$ fibroblasts were reversed by the neutralizing TGF-β antibody the signaling response to TGF-β was analyzed in further detail. Immunoblot analysis revealed increased SMAD2 phosphorylation (Fig. 6*A*) as evidenced by increased

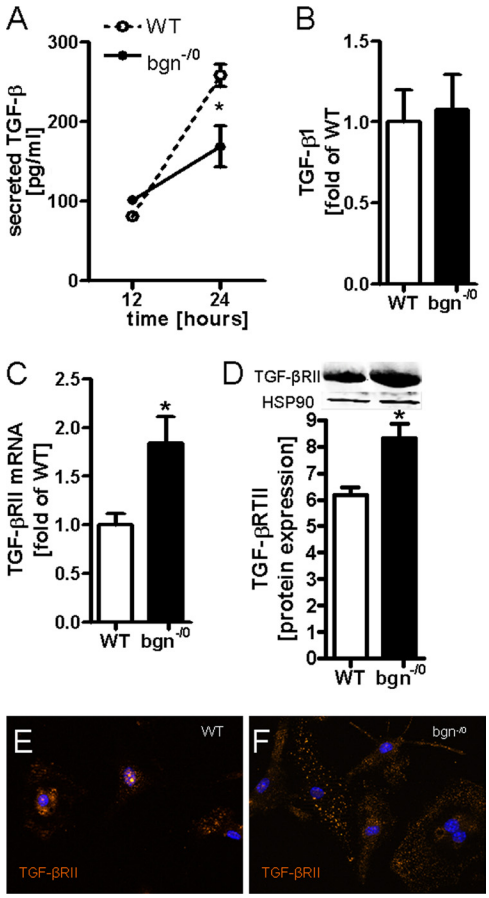

FIGURE 4. **Increased expression of TGF-βRII in bgn$^{-/0}$ fibroblasts.** *A*, TGF-β ELISA revealed lower levels of secreted TGF-β in medium conditioned by bgn$^{-/0}$ fibroblasts; $n = 3$. *B*, mRNA expression of TGF-β1 was not different between the two genotypes; $n = 6$. *C*, mRNA expression of TGF-βRII was significantly elevated in bgn$^{-/0}$ fibroblasts. *D*, immunoblotting of TGF-βRII; $n = 5$. *E* and *F*, immunocytochemical detection of TGF-βRII in primary cardiac fibroblasts in the first passage, representative images are shown of $n = 3$. The staining revealed increased TGF-βRII expression in bgn$^{-/0}$ fibroblasts. Analysis was performed 24 h after plating in 5% FCS. Data are presented as mean ± S.E.; *, $p < 0.05$.

ratio of phosphoSMAD2 and total SMAD2. Total SMAD2 was not changed (not shown). The data on SMAD2 phosphorylation therefore confirm increased TGF-β signaling in bgn$^{-/0}$ fibroblasts. In contrast SMAD3 phosphorylation was not consistently affected in bgn$^{-/0}$ fibroblasts (Fig. 6*B*). Importantly, ERK1/2 phosphorylation was enhanced in bgn$^{-/0}$ fibroblasts (Fig. 6*C*) corresponding to the proliferative advantage. Another target gene that is known to be induced by TGF-β is SMAD7. SMAD7 counteracts most common TGF-β responses as negative feedback. SMAD7 was significantly up-regulated in bgn$^{-/0}$ fibroblasts (Fig. 6*D*). Of note SMAD7 targets active TGF-βRI for degradation, which could be part of a negative feedback mechanism to balance the increased TGF-β response of bgn$^{-/0}$ fibroblasts. SMAD7 stabilizes β-catenin, which acts as transcription factor for c-Myc and p53 (44–46). In line with these known function of SMAD7, β-catenin showed significantly increased protein levels in bgn$^{-/0}$ fibroblasts (Fig. 6*E*). Of note, bgn$^{-/0}$ fibroblasts showed also increased apoptosis under normal conditions, as PARP1 cleavage was significantly increased in bgn$^{-/0}$ fibroblasts (Fig. 6*F*).

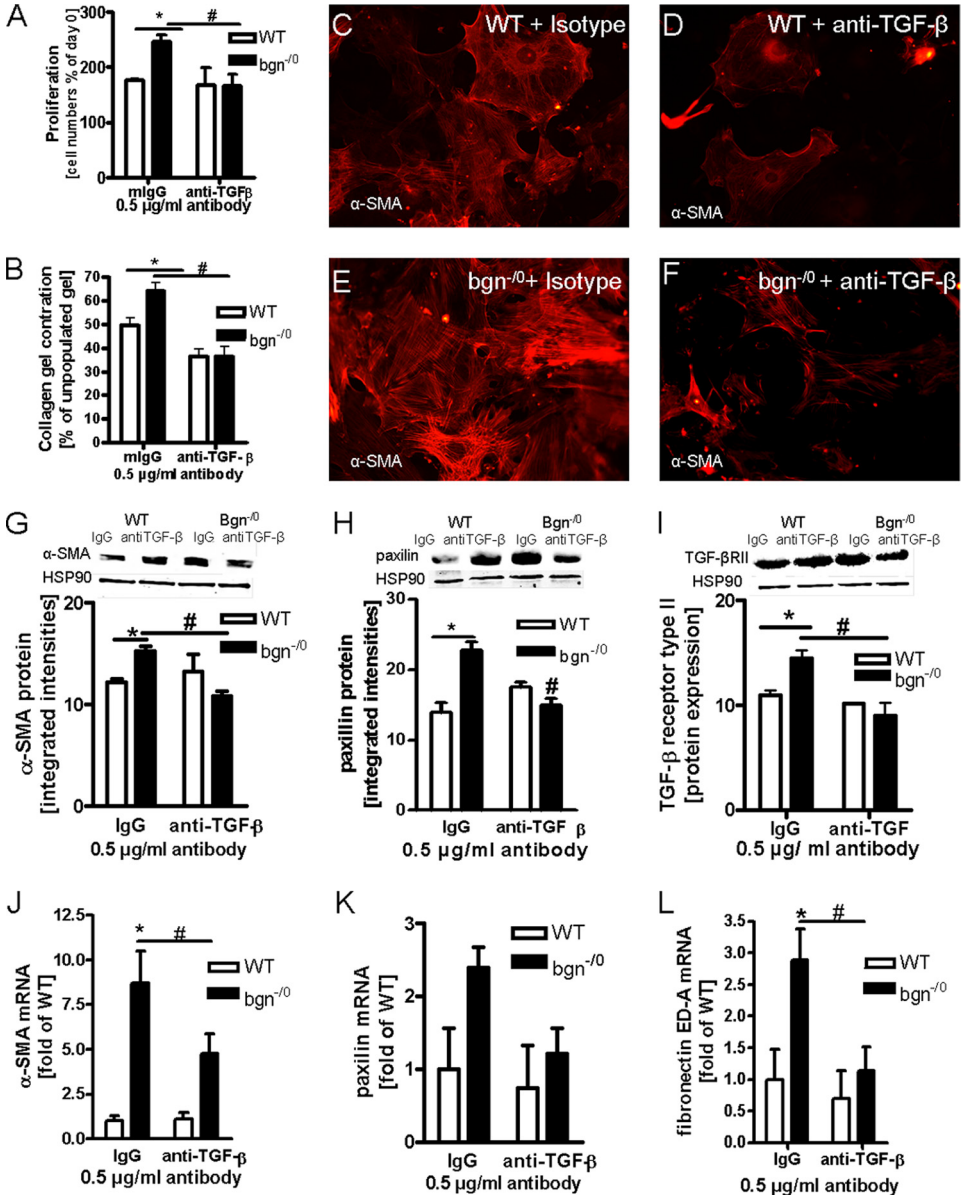

FIGURE 5. **Reversion of myofibroblast phenotype by neutralizing endogenous TGF-β.** *A*, cell growth in the presence of either non-immune mouse IgG (*mIgG*) as isotype control or neutralizing antibody to TGF-β -1, -2, -3 (anti-TGF-β) after 24 h in 5% FCS. Both antibodies were used at 0.5 μg/ml. Anti-TGF-β significantly inhibited proliferation of bgn$^{-/0}$ fibroblasts; $n = 3$. *B*, OSCR assay in the presence of mIgG or anti-TGF-β. Anti-TGFβ blocked enhanced collagen gel contraction by bgn$^{-/0}$ fibroblasts (*black bars*); $n = 3$. *C–F*, immunocytochemical staining of α-α-SMA of WT (*C* and *D*) and bgn$^{-/0}$ fibroblasts (*E* and *F*) treated with either mIgG (*C* and *E*) or anti-TGF-β neutralizing antibody (*D* and *F*). Anti-TGF-β reduced α-SMA-positive stress fibers in bgn$^{-/0}$ fibroblasts; 200× magnification; representative images of $n = 3$ experiments. *G*, immunoblotting confirmed the responsiveness of α-SMA to anti-TGFβ antibodies; $n = 3$. *H* and *I*, protein expression as evidenced by immunoblotting of paxillin (*H*) and TGF-βRII (*I*) were down-regulated by neutralization of TGF-β in bgn$^{-/0}$ fibroblasts as well. HSP90 served as loading control; $n = 3$. *J–L*, mRNA expression of α-SMA, paxillin, and the fibronectin fragment ED-A were analyzed by quantitative real-time PCR. α-SMA and fibronectin ED-A mRNA expression were increased in bgn$^{-/0}$ fibroblasts and were decreased by neutralizing TGF-β. Paxillin mRNA showed a similar trend; $n = 4$. Experiments were performed 24 h after plating in 5% FCS Data are presented as mean ± S.E.; $^{*,\#}$ $p < 0.05$.

Increased Myofibroblastic Response in bgn$^{-/0}$ Mice Post-MI—To test whether the myofibroblast phenotype develops also *in vivo* in bgn-deficient mice, experimental MI was performed. The mRNA expression of α-SMA was induced in WT hearts peaking 3 days after MI, which has been shown before to be the time of maximal myofibroblast appearance (10, 47) (Fig. 7*A*). After 3 days, α-SMA levels began to decline in WT mice, which is indicative for resolution of the myofibroblastic response. In bgn$^{-/0}$ mice mRNA expression of α-SMA was even more strongly increased than in WT hearts both 3 and 7 days post-MI (Fig. 7*A*). Next some of the key molecules that were affected by the bgn deletion in cardiac fibroblasts *in vivo* were analyzed in myocardial samples 3 days after MI. TGF-β1 mRNA (Fig. 7*B*) was significantly increased in bgn$^{-/0}$ hearts, where as TGF-β2 and 3 were not different between the two genotypes (data not shown). Furthermore, the mRNA of TGF-βRII and the myofibroblast marker fibronectin ED-A were increased in bgn$^{-/0}$ hearts after MI compared with WT (Fig. 7, *C* and *D*). As shown before *in vitro* the mRNA expression of SMAD7, CD44 and paxillin were increased in bgn$^{-/0}$ mice post-MI (Fig. 7, *E–G*).

Subsequently, the protein levels of α-SMA and TGF-βRII were found to be increased 3 days post-MI as evidenced by

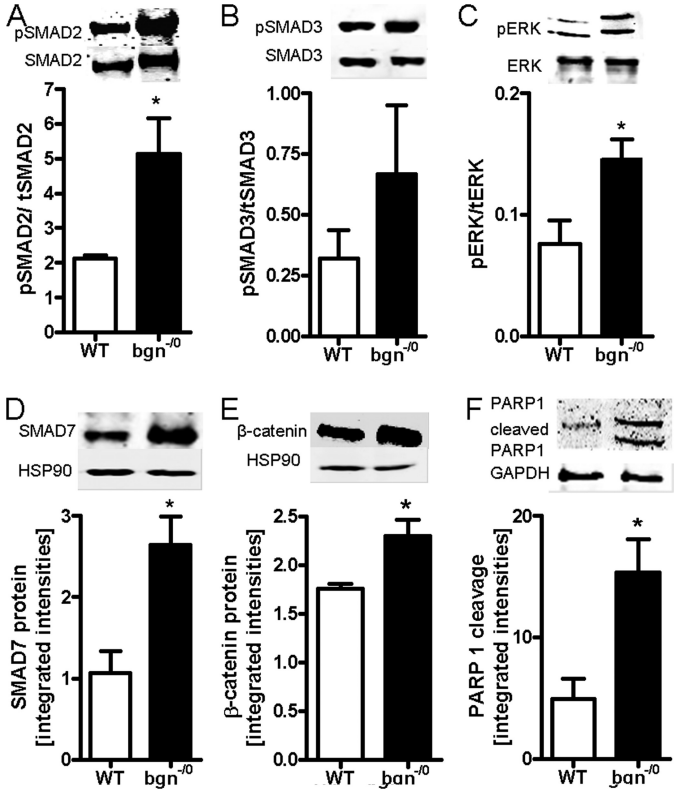

FIGURE 6. **Increased phosphorylation of SMAD2 and ERK in bgn$^{-/0}$ fibroblasts.** Cardiac fibroblasts were grown in 5% serum and Western blot analysis was performed 24 h after plating. *A–C*, immunoblotting and quantitative analysis of phosphorylated and total SMAD2 (*A*), SMAD3 (*B*), and ERK1/2 (*C*); $n = 3$. Quantitative data were expressed as the ratio between phosphorylated and total protein. *D* and *E*, SMAD7 and β-catenin expression were analyzed by Western blot and HSP90 protein was used as loading control for quantitative analysis; $n = 3$. *F*, PARP1 immunoblotting revealed increased PARP cleavage in bgn$^{-/0}$ fibroblasts but not in WT. GAPDH was used as loading control; $n = 9$. Data are presented as mean ± S.E.; *, $p < 0.05$.

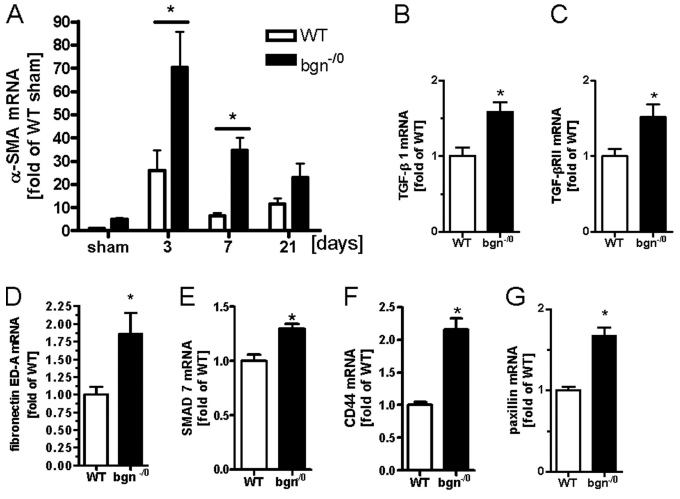

FIGURE 7. **Increased mRNA expression of α-SMA and myofibroblast-associated genes after experimental MI in bgn$^{-/0}$ mice.** Total RNA was isolated from the apex post-MI and analyzed for α-SMA, TGF-β1, TGF-βRII, fibronectin ED-A, SMAD7, CD44, and paxillin. mRNA expression as determined by quantitative real time RT-PCR and compared with results from sham-operated mice. *A*, α-SMA mRNA expression 3, 7, and 21 days postexperimental MI; $n = 7$(3 d), $n = 4$(7 d), $n = 9$ (21 d). *B–G*, mRNA expression of TGF-β1, TGF-βRII, fibronectin ED-A, SMAD7, CD44, and paxillin 3 days post-MI. Data are expressed as mean ± S.E.; *, $p < 0.05$; $n = 5$.

Western blotting. Indicative for increased TGF-β signaling the phosphorylation of SMAD2 was elevated in bgn$^{-/0}$ mice after MI and ERK1/2 phosphorylation showed only a trend to increased phosphorylation. Finally immunohistochemistry of α-SMA was performed to analyze the distribution of α-SMA cells. As shown in Fig. 8, *E–G* pronounced increase of α-SMA-positive cells were detected in the peri-infarct region 7 days post-MI. All considered the key differences between WT fibroblasts and bgn$^{-/0}$ fibroblasts pointing to a myofibroblastic phenotype in the absence of bgn were also observed *in vivo* post-MI.

DISCUSSION

Biglycan and decorin are differentially regulated after myocardial infarction. Furthermore genetic deletion of both SLRPs caused a distinct cardiac phenotype after experimental MI, characterized by disturbed remodeling and hemodynamic insufficiency (21, 22). These experiments revealed a more severe phenotype in bgn$^{-/0}$ compared with decorin$^{-/-}$ mice, as evidenced by rupture of infarct scars and increased mortality in bgn$^{-/0}$ mice. Mechanistically it was demonstrated that the collagenous network of the infarct scars was distorted explaining the rupture phenotype. In the present study it was addressed whether the deletion of bgn affects the phenotype of cardiac fibroblasts, *in vitro*, which may contribute to the phenotype after MI *in vivo*.

In the first sets of the experiments, a pro-proliferative phenotype of bgn$^{-/0}$ fibroblasts was demonstrated that was clearly caused by the lack of bgn in the pericellular ECM, because WT-ECM, addition of purified recombinant BGN and overexpression of bgn rescued this phenotype. This is in line with results in various other cell types. Bgn inhibits the proliferation of endothelial cells (48), of osteogenic precursors and pancreatic cancer cells (49, 50). It was also demonstrated that soluble bgn inhibits PDGF-BB-induced proliferation in mesanglial cells (51). In contrast, overexpression of bgn in smooth muscle cells supported proliferation (48). Therefore, it appears that the effect of bgn on proliferation may be cell type-specific. It has been shown that increased ability of fibroblasts to contract collagen gels is due to differentiation into myofibroblasts (40, 52, 53). Accordingly, in addition to the pro-proliferative phenotype, the morphology, and behavior of bgn$^{-/0}$ fibroblasts resembled a myofibroblast phenotype as evidenced by increased α-SMA incorporation into stress fibers and increased collagen gel contraction. In line with these findings increased formation of focal adhesions occurred in bgn$^{-/0}$ fibroblasts and expression of fibronectin ED-A was up-regulated. This is the first evidence that bgn is a regulator of myofibroblast differentiation. With respect to the other SLRPs it has been suggested that at least decorin may have similar effects, as decorin inhibits TGF-β-induced contraction and basal contraction of smooth muscle cells, hypertrophic scar fibroblasts and embryonic fibroblasts (54–56). Furthermore, it was shown that embryonic fibroblasts from decorin-null mice show stronger contractile abilities under static tension than WT fibroblasts, which in part is reversed by TGF-β treatment (55).

In search of the underlying mechanism, it was found in the present study that TGF-βRII expression and SMAD2 phosphor-

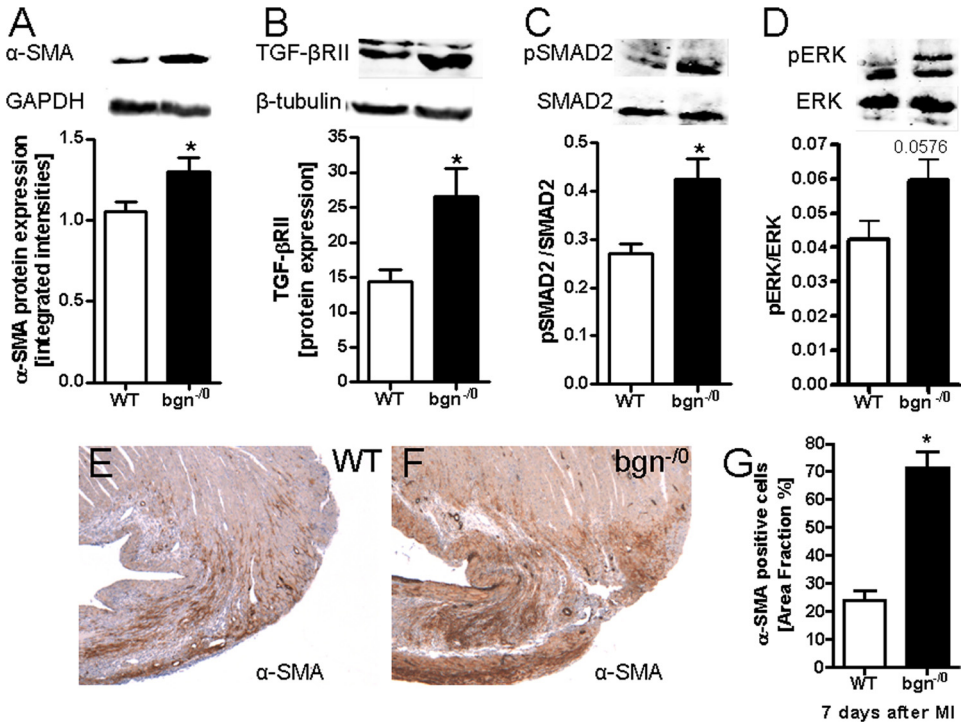

FIGURE 8. **TGF-βRII protein expression and SMAD2 phosphorylation were increased post-MI in bgn$^{-/0}$ mice.** Immunoblotting using left ventricular tissue extracts 3 days post-MI. *A*, Western blotting of α-SMA in tissue extracts from infarcted ventricles confirmed increased α-SMA expression in bgn$^{-/0}$ mice. *B*, TGF-βRII protein expression. *C*, increased ratio of phosphorylated SMAD2 to total SMAD2 in bgn$^{-/0}$ hearts. *D*, ratio of phosphorylated ERK to total ERK1/2 revealed only a trend toward increased phosphorylation of ERK1/2; in *A–D*, $n = 5$. *E* and *F*, immunostaining of α-SMA 7 days after experimental MI. Shown are representative images of the peri-infarct zone confirming up-regulated α-SMA expression in bgn$^{-/0}$ mice; $n = 4$. *G*, quantification of α-SMA immunohistochemistry as in *D* and *E* was performed using ImageJ (NIH). Data are expressed as mean ± S.E.; *, $p < 0.05$.

ylation were increased despite of slightly lower TGF-β concentration in the supernatants. Furthermore, blocking TGF-β by neutralizing antibodies reversed the phenotypic hallmarks of bgn$^{-/0}$ fibroblasts such as the pro-proliferative phenotype, α-SMA expression, focal adhesions, collagen gel contraction, and fibronectin ED-A expression. These results strongly suggested that endogenous TGF-β signaling may be enhanced and that TGF-β signaling was responsible for the myofibroblast phenotype. TGF-β initially binds to TGF-βRII, which then recruits and phosphorylates TGF-βRI (57). This receptor complex than recruits cofactors such as SARA and receptor-regulated SMADs, which are phosphorylated by TGF-βRI upon ligand binding. SMAD signaling can be transduced by heterodimer and homodimers of SMAD2 and SMAD3. In addition active SMAD2 interacts with SMURF2 an E2 ubiquitin ligase, and this complex leads to degradation of transcription inhibitors such as Ski and SnoN (58, 59). In the present study, increased SMAD2 phosphorylation was sensitive to blocking TGF-β1 antibodies. In line with the present results myofibroblasts of human epiretinal membranes show increased TGF-βRII expression (60). Furthermore, bgn and fibromodulin double-deficient mandibular condylar chondrocytes have overactive TGF-β signaling leading to chondrogenesis and ECM turn over (17, 61). Therefore, the present findings are in line with the literature on SLRPs suggesting that lack of SLRPs may in certain biological context enhance TGF-β signaling. Specifically, in cardiac fibroblasts the present data suggest that lack of bgn causes a myofibroblast phenotype by increased TGF-βRII expression and SMAD2 signaling.

However, the phenotype of bgn$^{-/0}$ fibroblasts appears to be more complex, due to the fact that increased SMAD7 and β-catenin levels were detected as well, which might be the cause of yet another facet of this phenotype. SMAD7 is translocated into the cytosol upon TGF-β signaling and then stabilizes β-catenin binding to E-cadherin complexes. In turn, these complexes inhibit phosphorylation of β-catenin and thereby its degradation (62). Furthermore, SMAD 7 interacts with β-catenin to modulate TGF-β induced apoptosis, as SMAD7 acts as positive regulator of the TGF-β-activated pathway involving TAK1-MKK3 and p38 mitogen-activated kinases, leading to induction of c-Myc and p53 and subsequently apoptosis (46, 62–64). Indeed, increased apoptosis was detected by PARP1 cleavage, despite of the proliferative phenotype. This could be part of a negative feed back mechanism to balance the increased proliferative rate of bgn$^{-/0}$ fibroblasts. In mesanglial cells, it was demonstrated that soluble bgn inhibited cyclohexamide-induced apoptosis (51). In 2002, Young *et al.* showed that bgn-deficient mice have diminished capacity to produce bone marrow stromal cells (BMSCs), and that these cells are characterized by more apoptosis than cells from normal control littermates. Furthermore, bgn and decorin double-deficient BMSCs undergo apoptosis more often than WT BMSCs (65).

CD44 was up-regulated in bgn$^{-/0}$ fibroblast *in vitro*. This is of interest because in CD44-null mice, fibroblast infiltration, myofibroblast differentiation, and matrix production in the infarct zone is markedly reduced, while inflammation is increased leading to increased ventricular dilation (42). Furthermore, less SMAD2 phosphorylation and decreased prolif-

eration was detected in CD44-null mice compared with WT mice (42). These findings implicated CD44 via SMAD2 signaling in myofibroblast differentiation and function. It is therefore conceivable that the up-regulation of CD44 in the absence of biglycan, as described here, supports the increased TGF-β 1 response and the pro-proliferative myofibroblast phenotype of the bgn$^{-/0}$ fibroblasts.

The changes in the TGF-β system were paralleled by induction of PLOD1, PLOD2 and MMP13 in bgn$^{-/0}$ fibroblasts, which is in line with the myofibroblastic phenotype and suggests that bgn$^{-/0}$ fibroblasts showed differences with respect to matrix remodeling. These results are also in line with the increased expression of MMP13 in bgn$^{-/0}$ hearts *in vivo* after MI as described earlier (22). During the first 48 h post-MI, macrophages infiltrate the infarcted area and secrete cytokines and growth factors, such as TGF-β, leading to the appearance of myofibroblasts (12). Importantly, the myofibroblast phenotype of bgn$^{-/0}$ fibroblasts reported here *in vitro* was also detected *in vivo*. Namely, increased α-SMA and other key changes observed *in vitro* occurred also in infarcted hearts of bgn$^{-/0}$ mice at 3 and 7 days post-MI. Because in WT mice, myofibroblasts decline at the time when bgn accumulates in the peri-infarct area (22), it may be hypothesized that bgn functions as a molecular switch to terminate the myofibroblastic response.

In summary, it is shown here for the first time that the lack of bgn causes cardiac fibroblasts to differentiate into pro-proliferative myofibroblasts due to increased sensitivity to endogenous TGF-β/SMAD2 signaling. Myofibroblast contraction of the scar leads to scar thinning, and increased wall tension may contribute to ventricular stiffness and diastolic dysfunction (12). Therefore, increased myofibroblast differentiation in the absence of bgn may be involved in the cardiac phenotype of bgn$^{-/0}$ mice post-MI which was characterized by hemodynamic dysfunction and ventricular ruptures. As a working hypothesis to explain the phenotype of bgn$^{-/0}$ mice post-MI, it may be considered that biglycan causes distortion of collagen fibril assembly in the scar as shown by Westermann *et al.* (22). In addition the lack of bgn may cause increased scar contraction by myofibroblasts as suggested here. Together these two mechanisms may cause decreased stability and increased tension and therefore increased susceptibility of the scar to rupture. The function of bgn during fibroblast phenotype regulation might also be important to consider in response to various pharmacologic treatments that affect bgn expression and deposition such, as angiotensin II receptor type 1 antagonists or statins (66, 67).

REFERENCES

1. Zamilpa, R., and Lindsey, M. L. (2010) *J. Mol. Cell Cardiol.* **48,** 558–563
2. Berschneider, H. M. (1992) *Ann. N. Y. Acad. Sci.* **664,** 140–147
3. Berschneider, H. M., and Powell, D. W. (1992) *J. Clin. Invest.* **89,** 484–489
4. Hinterleitner, T. A., Saada, J. I., Berschneider, H. M., Powell, D. W., and Valentich, J. D. (1996) *Am. J. Physiol.* **271,** C1262–C1268
5. Tomasek, J. J., Gabbiani, G., Hinz, B., Chaponnier, C., and Brown, R. A. (2002) *Nat. Rev. Mol. Cell Biol.* **3,** 349–363
6. Wilborn, J., Crofford, L. J., Burdick, M. D., Kunkel, S. L., Strieter, R. M., and Peters-Golden, M. (1995) *J. Clin. Invest.* **95,** 1861–1868
7. Wilborn, J., DeWitt, D. L., and Peters-Golden, M. (1995) *Am. J. Physiol.* **268,** L294–L301
8. Porter, K. E., and Turner, N. A. (2009) *Pharmacol. Ther.* **123,** 255–278
9. Welch, M. P., Odland, G. F., and Clark, R. A. (1990) *J. Cell Biol.* **110,** 133–145
10. Sun, Y., and Weber, K. T. (1996) *J. Mol. Cell Cardiol.* **28,** 851–858
11. Desmoulière, A., Redard, M., Darby, I., and Gabbiani, G. (1995) *Am. J. Pathol.* **146,** 56–66
12. Sun, Y., and Weber, K. T. (2000) *Cardiovasc. Res.* **46,** 250–256
13. Tiede, K., Melchior-Becker, A., and Fischer, J. W. (2010) *Basic Res. Cardiol.* **105,** 99–108
14. Corsi, A., Xu, T., Chen, X. D., Boyde, A., Liang, J., Mankani, M., Sommer, B., Iozzo, R. V., Eichstetter, I., Robey, P. G., Bianco, P., and Young, M. F. (2002) *J. Bone Miner. Res.* **17,** 1180–1189
15. Danielson, K. G., Baribault, H., Holmes, D. F., Graham, H., Kadler, K. E., and Iozzo, R. V. (1997) *J. Cell Biol.* **136,** 729–743
16. Reinboth, B., Hanssen, E., Cleary, E. G., and Gibson, M. A. (2002) *J. Biol. Chem.* **277,** 3950–3957
17. Hildebrand, A., Romaris, M., Rasmussen, L. M., Heinegard, D., Twardzik, D. R., Border, W. A., and Ruoslahti, E. (1994) *Biochem. J.* **302,** 527–534
18. Schaefer, L., Babelova, A., Kiss, E., Hausser, H. J., Baliova, M., Krzyzankova, M., Marsche, G., Young, M. F., Mihalik, D., Götte, M., Malle, E., Schaefer, R. M., and Gröne, H. J. (2005) *J. Clin. Invest.* **115,** 2223–2233
19. Kitaya, K., and Yasuo, T. (2009) *J. Leukoc. Biol.* **85,** 391–400
20. Webber, J., Jenkins, R. H., Meran, S., Phillips, A., and Steadman, R. (2009) *Am. J. Pathol.* **175,** 148–160
21. Weis, S. M., Zimmerman, S. D., Shah, M., Covell, J. W., Omens, J. H., Ross, J., Jr., Dalton, N., Jones, Y., Reed, C. C., Iozzo, R. V., and McCulloch, A. D. (2005) *Matrix Biol.* **24,** 313–324
22. Westermann, D., Mersmann, J., Melchior, A., Freudenberger, T., Petrik, C., Schaefer, L., Lüllmann-Rauch, R., Lettau, O., Jacoby, C., Schrader, J., Brand-Herrmann, S. M., Young, M. F., Schultheiss, H. P., Levkau, B., Baba, H. A., Unger, T., Zacharowski, K., Tschöpe, C., and Fischer, J. W. (2008) *Circulation* **117,** 1269–1276
23. Campbell, P. H., Hunt, D. L., Jones, Y., Harwood, F., Amiel, D., Omens, J. H., and McCulloch, A. D. (2008) *Mol. Cell Biomech.* **5,** 27–35
24. Xu, T., Bianco, P., Fisher, L. W., Longenecker, G., Smith, E., Goldstein, S., Bonadio, J., Boskey, A., Heegaard, A. M., Sommer, B., Satomura, K., Dominguez, P., Zhao, C., Kulkarni, A. B., Robey, P. G., and Young, M. F. (1998) *Nat. Genet.* **20,** 78–82
25. Rock, K., Fischer, K., and Fischer, J. W. (2010) *Dermatology*, in press
26. Peterkofsky, B. (1972) *Biochem. Biophys. Res. Commun.* **49,** 1343–1350
27. Schwarz, R. I., and Bissell, M. J. (1977) *Proc. Natl. Acad. Sci. U.S.A.* **74,** 4453–4457
28. Zern, M. A., Schwartz, E., Giambrone, M. A., and Blumenfeld, O. O. (1985) *Exp. Cell Res.* **160,** 307–318
29. Mann, B. K., Schmedlen, R. H., and West, J. L. (2001) *Biomaterials* **22,** 439–444
30. Jones, P. A., Scott-Burden, T., and Gevers, W. (1979) *Proc. Natl. Acad. Sci. U.S.A.* **76,** 353–357
31. Masters, K. S., Lipke, E. A., Rice, E. E., Liel, M. S., Myler, H. A., Zygourakis, C., Tulis, D. A., and West, J. L. (2005) *J. Biomater. Sci. Polym. Ed.* **16,** 659–672
32. Leurs, C., Jansen, M., Pollok, K. E., Heinkelein, M., Schmidt, M., Wissler, M., Lindemann, D., Von Kalle, C., Rethwilm, A., Williams, D. A., and Hanenberg, H. (2003) *Hum. Gene Ther.* **14,** 509–519
33. Kalmes, M., Neumeyer, A., Rio, P., Hanenberg, H., Fritsche, E., and Blömeke, B. (2006) *Biol. Chem.* **387,** 1201–1207
34. Dai, G., Freudenberger, T., Zipper, P., Melchior, A., Grether-Beck, S., Rabausch, B., de Groot, J., Twarock, S., Hanenberg, H., Homey, B., Krutmann, J., Reifenberger, J., and Fischer, J. W. (2007) *Am. J. Pathol.* **171,** 1451–1461
35. Kresse, H., Liszio, C., Schönherr, E., and Fisher, L. W. (1997) *J. Biol. Chem.* **272,** 18404–18410
36. Kresse, H., Seidler, D. G., Muller, M., Breuer, E., Hausser, H., Roughley, P. J., and Schonherr, E. (2001) *J. Biol. Chem.* **276,** 13411–13416
37. Schaefer, L., Mihalik, D., Babelova, A., Krzyzankova, M., Gröne, H. J., Iozzo, R. V., Young, M. F., Seidler, D. G., Lin, G., Reinhardt, D. P., and Schaefer, R. M. (2004) *Am. J. Pathol.* **165,** 383–396
38. Vernon, R. B., and Gooden, M. D. (2002) *In Vitro Cell Dev. Biol. Anim.* **38,** 97–101

39. Dobaczewski, M., Bujak, M., Zymek, P., Ren, G., Entman, M. L., and Frangogiannis, N. G. (2006) *Cell Tissue Res.* **324,** 475–488
40. Hinz, B. (2007) *J. Invest. Dermatol.* **127,** 526–537
41. Acharya, P. S., Majumdar, S., Jacob, M., Hayden, J., Mrass, P., Weninger, W., Assoian, R. K., and Puré, E. (2008) *J. Cell Sci.* **121,** 1393–1402
42. Huebener, P., Abou-Khamis, T., Zymek, P., Bujak, M., Ying, X., Chatila, K., Haudek, S., Thakker, G., and Frangogiannis, N. G. (2008) *J. Immunol.* **180,** 2625–2633
43. Yu, Q., and Stamenkovic, I. (2000) *Genes Dev.* **14,** 163–176
44. Mazars, A., Lallemand, F., Prunier, C., Marais, J., Ferrand, N., Pessah, M., Cherqui, G., and Atfi, A. (2001) *J. Biol. Chem.* **276,** 36797–36803
45. Edlund, S., Bu, S., Schuster, N., Aspenström, P., Heuchel, R., Heldin, N. E., ten Dijke, P., Heldin, C. H., and Landström, M. (2003) *Mol. Biol. Cell* **14,** 529–544
46. Landström, M., Heldin, N. E., Bu, S., Hermansson, A., Itoh, S., ten Dijke, P., and Heldin, C. H. (2000) *Curr. Biol.* **10,** 535–538
47. Willems, I. E., Havenith, M. G., De Mey, J. G., and Daemen, M. J. (1994) *Am. J. Pathol.* **145,** 868–875
48. Shimizu-Hirota, R., Sasamura, H., Kuroda, M., Kobayashi, E., Hayashi, M., and Saruta, T. (2004) *Circ. Res.* **94,** 1067–1074
49. Weber, C. K., Sommer, G., Michl, P., Fensterer, H., Weimer, M., Gansauge, F., Leder, G., Adler, G., and Gress, T. M. (2001) *Gastroenterology* **121,** 657–667
50. Inkson, C. A., Ono, M., Bi, Y., Kuznetsov, S. A., Fisher, L. W., and Young, M. F. (2009) *Cells Tissues Organs* **189,** 153–157
51. Schaefer, L., Beck, K. F., Raslik, I., Walpen, S., Mihalik, D., Micegova, M., Macakova, K., Schonherr, E., Seidler, D. G., Varga, G., Schaefer, R. M., Kresse, H., and Pfeilschifter, J. (2003) *J. Biol. Chem.* **278,** 26227–26237
52. Lijnen, P., Petrov, V., and Fagard, R. (2003) *J. Renin. Angiotensin Aldosterone Syst.* **4,** 113–118
53. Lijnen, P., Petrov, V., Rumilla, K., and Fagard, R. (2003) *Methods Find Exp. Clin. Pharmacol.* **25,** 79–86
54. Järveläinen, H., Vernon, R. B., Gooden, M. D., Francki, A., Lara, S., Johnson, P. Y., Kinsella, M. G., Sage, E. H., and Wight, T. N. (2004) *Arterioscler. Thromb. Vasc. Biol.* **24,** 67–72
55. Ferdous, Z., Wei, V. M., Iozzo, R., Höök, M., and Grande-Allen, K. J. (2007) *J. Biol. Chem.* **282,** 35887–35898
56. Zhang, Z., Garron, T. M., Li, X. J., Liu, Y., Zhang, X., Li, Y. Y., and Xu, W. S. (2009) *Burns.* **35,** 527–537
57. Wrana, J. L., Attisano, L., Wieser, R., Ventura, F., and Massagué, J. (1994) *Nature* **370,** 341–347
58. Bonni, S., Wang, H. R., Causing, C. G., Kavsak, P., Stroschein, S. L., Luo, K., and Wrana, J. L. (2001) *Nat. Cell Biol.* **3,** 587–595
59. Cunnington, R. H., Nazari, M., and Dixon, I. M. (2009) *Can. J. Physiol. Pharmacol.* **87,** 764–772
60. Bochaton-Piallat, M. L., Kapetanios, A. D., Donati, G., Redard, M., Gabbiani, G., and Pournaras, C. J. (2000) *Invest. Ophthalmol. Vis. Sci.* **41,** 2336–2342
61. Embree, M. C., Kilts, T. M., Ono, M., Inkson, C. A., Syed-Picard, F., Karsdal, M. A., Oldberg, A., Bi, Y., and Young, M. F. (2010) *Am. J. Pathol.* **176,** 812–826
62. Tang, Y., Liu, Z., Zhao, L., Clemens, T. L., and Cao, X. (2008) *J. Biol. Chem.* **283,** 23956–23963
63. Edlund, S., Lee, S. Y., Grimsby, S., Zhang, S., Aspenström, P., Heldin, C. H., and Landström, M. (2005) *Mol. Cell Biol.* **25,** 1475–1488
64. Ebisawa, T., Fukuchi, M., Murakami, G., Chiba, T., Tanaka, K., Imamura, T., and Miyazono, K. (2001) *J. Biol. Chem.* **276,** 12477–12480
65. Young, M. F., Bi, Y., Ameye, L., and Chen, X. D. (2002) *Glycoconj J.* **19,** 257–262
66. Marzoll, A., Melchior-Becker, A., Cipollone, F., and Fischer, J. W. (2009) *J. Cell Mol. Med.*, in press
67. Nagy, N., Melchior-Becker, A., and Fischer, J. W. (2010) *Basic Res. Cardiol.* **105,** 29–38